NEW QCD EFFECTS AT LARGE x*

P. Hoyer

Department of Physics
University of Helsinki, Helsinki, Finland

In heavy quark production at large Feynman x there are two hardness scales, one given by the heavy quark pair mass $\mathcal{M}^2$ and the other by $\Lambda_{QCD}^2/(1-x)$. When these two scales are comparable, the twist expansion of Perturbative QCD breaks down. We discuss the dynamics in this new QCD limit, where $\mu^2 = \mathcal{M}^2(1-x)$ is held fixed as $\mathcal{M}^2 \to \infty$. New diagrams are found to contribute, which can enhance the cross section above that expected for leading twist. The heavy quarks are produced by a peripheral scattering on the target of hardness μ^2. This leads, in particular, to a nuclear target dependence of $A^{2/3}$ at small μ. Qualitatively, the dynamics in the new limit agrees with earlier phenomenological models of "intrinsic" heavy quark production.

PACS numbers: 12.38. Bx

1. Introduction

The application of Perturbative QCD (PQCD) to hard processes involving hadrons and leptons has been very successful. The predictive power of PQCD is based on the factorization theorem [1], according to which an observable cross section σ can be factorized into a product of universal structure and fragmentation functions times the hard constituent cross section $\hat{\sigma}$. Generically,

$$\sigma = F_a F_b \, \hat{\sigma}(ab \to c + X)D_c \,, \tag{1.1}$$

where F_a, F_b are the single parton structure functions of the incoming hadrons ("probabilities for finding the quarks/gluons a, b in the projectile and target") and D_c describes the hadronization of the produced quark(s)/gluon(s) c into the observed final state (*e.g.*, jets or hadrons at

---

large $p_\perp$). The structure and fragmentation functions F, D are not calculable in PQCD, but are predicted to be *universal*, *i.e.*, independent of the specific hard collision $\hat{\sigma}$. The "higher twist" corrections to the "leading twist" PQCD prediction (1) are suppressed by powers of the large momentum scale Q^2, which characterizes the hard subprocess ab $\to$ c $+ X$.

Here I would like to discuss modifications to Eq. (1.1) that are expected, and observed, in the case that one of the partons a, b or c carries a large fraction x of the available longitudinal momentum. In the $x \to 1$ limit there is a new hard scale $\Lambda_{QCD}^2/(1 - x)$, and the corrections to Eq. (1.1) are of order $\Lambda_{QCD}^2/Q^2(1 - x)$. In the combined limit

$$\left. \begin{array}{c} Q^2 \to \infty \\[2mm] x \to 1 \end{array} \right\} \quad \text{with } \mu^2 = Q^2(1 - x) \text{ fixed}, \qquad (1.2)$$

the twist expansion in fact breaks down [2]. The higher twist contributions are of $\mathcal{O}(1/\mu^2)$, and hence not suppressed by an asymptotically large variable in this new QCD limit. Since large momentum transfers are involved, PQCD can still be used to analyze the process. As I shall discuss below, in this limit the cross section cannot be expressed in terms of single-parton structure functions; it involves multiparton distributions. This is similar to the case of exclusive ($x = 1$) hard scattering, which depends on the longitudinal momentum distributions of all (valence) quarks, constrained to be at small transverse distances from each other [3].

2. Why the $x \to 1$ limit is hard

Consider the wave function $\phi(yp, \vec{n}_\perp)$ of the hadron h in Fig. 1, in a frame where h has a large longitudinal momentum p. We shall assume that ϕ describes the soft, non-perturbative part of the quark distributions, and is suppressed in the limits $y \to 0, 1$ and also for $n_\perp \to \infty$. The perturbative tail of the full wave function[1] when the fractional momentum of one constituent $x \to 0, 1$ or when its transverse momentum $p_\perp \to \infty$ is then generated by gluon exchange as shown in Fig. 1.

It is in fact straightforward to see [2] that Fock states where one constituent carries a large momentum fraction $x \simeq 1$ must have a short life-time, and hence are calculable in PQCD. The (kinetic) energy difference between the final Fock state of Fig. 1 and the hadron is

$$\Delta E_{q\bar{q}} \equiv E_h - E_{q\bar{q}} = \sqrt{p^2 + m_h^2} - \sum_i \sqrt{(x_i p)^2 + p_\perp^2 + m_q^2}$$

---

[1] The following simplified discussion ignores multiple gluon exchanges, which will bring logarithmic corrections, in analogy to the treatment in Ref. [3].

$$\simeq \frac{1}{2p}\left[m_h^2 - \frac{m_q^2 + p_\perp^2}{x(1-x)}\right] \propto \frac{1}{1-x}, \tag{2.1}$$

where we assumed $p \gg p_\perp/(1-x)$. By the uncertainty principle the "life-time" $\tau_{q\bar{q}}$ of the Fock state is then proportional to $1 - x$:

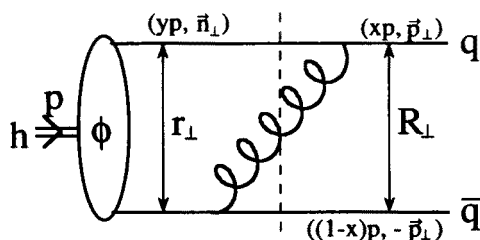$$\tau_{q\bar{q}} \simeq \frac{1}{\Delta E} \simeq \frac{2px}{m_q^2 + p_\perp^2}(1-x). \tag{2.2}$$

Fig. 1. The $x \to 1$ limit of a hadron structure function is generated by perturbative gluon exchange. The transverse size $r_\perp$ of the initial Fock state is small, $r_\perp^2 \sim (1-x)/p_\perp^2$. The virtual state with large x has a larger size $R_\perp \sim 1/p_\perp$, due to the transverse motion of the stopped quark carrying the small momentum fraction $1 - x$.

Furthermore, since the life-time of the $x \to 1$ Fock state is brief, we would expect that the transverse distance $r_\perp$ in Fig. 1, between the quarks before/during the gluon exchange must be similarly short, so that the duration of the exchange is no longer than the life-time $\tau_{q\bar{q}}$. This is readily verified because the gluon exchange amplitude depends on the constituent transverse momentum $\vec{n}_\perp$ only through the energy difference associated with the dashed line in Fig. 1,

$$2p\Delta E \simeq \frac{m_q^2 + n_\perp^2}{1-y} - \frac{m_q^2 + p_\perp^2}{1-x} - \frac{(\vec{n}_\perp - \vec{p}_\perp)^2}{x-y}. \tag{2.3}$$

For $x \to 1$, ΔE is independent of $n_\perp$ for

$$n_\perp^2 \lesssim \mathcal{O}\left(\frac{p_\perp^2}{1-x}\right). \tag{2.4}$$

Since the non-perturbative wave function ϕ of the hadron will cut off the integration over $\vec{n}_\perp$ before the limit (2.4) is reached, the $n_\perp$-integration can be factorized,

$$\int d\vec{n}_\perp \phi(yp, \vec{n}_\perp) = \phi(yp, r_\perp = 0), \tag{2.5}$$

showing that the only hadronic Fock states which can generate the $x \to 1$ perturbative tail are those with a short transverse distance $r_\perp^2 \propto 1 - x$ between the quarks. Conversely, according to Eq. (2.4) the $x \to 1$ Fock states involve large transverse momenta $n_\perp^2 \propto 1/(1 - x)$.

It is important to note that the $x \to 1$ Fock state, which is compact at its moment of creation, nevertheless quickly expands in the transverse direction. During the effective life-time (2.2) of the Fock state, the "slow" quark can move a transverse distance

$$R_\perp \simeq v_\perp \tau_{\mathrm{q\bar{q}}} = \frac{p_\perp}{p(1 - x)} \frac{2px}{m_{\mathrm{q}}^2 + p_\perp^2}(1 - x) \simeq \frac{2p_\perp x}{m_{\mathrm{q}}^2 + p_\perp^2} \qquad (2.6)$$

which for $p_\perp = \mathcal{O}(\Lambda_{\mathrm{QCD}})$ is of the order of 1 fm. This observation will be important in the following.

Because of the hard scale (2.4), PQCD can be used to calculate the behavior of hadronic structure functions in the $x \to 1$ limit. The result is given by the "spectator counting rules" [4–6]

$$\frac{dF}{dx} \propto (1 - x)^{2n_s - 1 + 2|\Delta\lambda|}, \qquad (2.7)$$

where n_s is the number of "spectator" partons (whose $x_s \to 0$) and $\Delta\lambda$ is the helicity flip between the initial hadron and the observed quark (or gluon) carrying the large momentum fraction x.

3. Breakdown of the twist expansion for $x \to 1$

Consider the well-known process of Deep Inelastic Scattering (DIS) of leptons on hadrons. The diagrams are classified as "Leading Twist" (Fig. 2(a)) or "Higher Twist" (HT, Fig. 2(b)) according to whether the spectator partons in the target are, or are not, connected to the active (hit) quark (or to partons radiated from this active quark).

In the $Q^2 \to \infty$ (fixed x) limit, the HT diagrams are suppressed by $1/Q^2$. This can be intuitively understood as follows. The hard $\ell q \to \ell' q$ subprocess has a duration $\tau \sim 1/Q$. Any interaction with spectators as in Fig. 2(b) can affect the hard scattering probability only if it occurs within this short time interval τ (later interactions will only modify the momentum distribution of the struck quark in the final state). But an interaction within a time-scale τ is possible only if there are spectators within a transverse distance $r_\perp \sim \tau \sim 1/Q$. The probability for this is proportional to the transverse area $\pi r_\perp^2 \sim 1/Q^2$, which explains the suppression of the higher twist contributions.

The above argument for the suppression of HT terms breaks down in the high x limit. As we argued earlier, the $x \to 1$ Fock states in Fig. 1
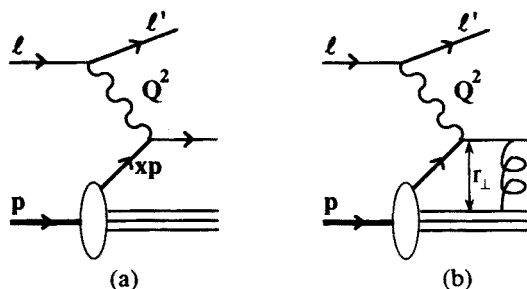
Fig. 2. Deep inelastic lepton-hadron scattering. (a) A leading twist diagram. (b) A higher twist diagram.

are produced from compact hadron configurations, with a typical distance $r_\perp^2 \sim (1-x)/\mu^2$ between the valence quarks, where $\mu \sim 1$ fm^{-1}. Hence in DIS with $Q^2 \sim \mu^2/(1-x)$, *i.e.*, in the limit (1.2), the scale of the hard photon interaction is commensurate with the size of the valence Fock state, and the scattering is coherent over several quarks. This means that the DIS cross section cannot be expressed in terms of single-parton structure functions in the limit (1.2), and the usual factorization (1.1) fails.

The magnitude of the higher twist terms has been studied experimentally in DIS as a function of x. The results show [7] that the HT corrections are important for $x \gtrsim 0.5$, and have an x-dependence which is consistent with $(1-x)^{-1}$, as suggested by the above qualitative arguments and explicit calculations [1, 5, 8]. Similarly, in high mass lepton pair production there is experimental evidence [9, 10] for corrections to the Drell–Yan process, which are in qualitative agreement with the expectations for higher twist effects [11].

4. Dynamics in the new QCD limit

We have studied [2] the production of quark pairs with large invariant mass $\mathcal{M}$ in the high x limit corresponding to (1.2), *i.e.*, for

$$\left. \begin{array}{c} \mathcal{M}^2 \to \infty \\ x \to 1 \end{array} \right\} \quad \text{with } \mu^2 = \mathcal{M}^2(1-x) \text{ fixed}, \quad (4.1)$$

where x is the momentum fraction of the $q\bar{q}$ system. An explicit calculation of all relevant diagrams was done for scalar QED. Here I would like to discuss the qualitative conclusions, which apply equally to QCD.

Consider first heavy quark production in the standard QCD limit,

$$\mathcal{M}^2 \to \infty \quad \text{at fixed } x. \quad (4.2)$$

The usual lowest order diagram describing the fusion process $GG \rightarrow Q\bar{Q}$ is shown in Fig. 3(a). The virtualities of both gluons range up to $\mathcal{O}(\mathcal{M}^2)$ – their momentum distributions are given by the projectile and target gluon structure functions evaluated at a scale $Q^2 = \mathcal{M}^2$. Similarly in Fig. 3(b), the higher order (in α_s) process $\bar{q}G \rightarrow \bar{q}Q\bar{Q}$ is given by the antiquark and gluon structure functions of the projectile and target, respectively, evaluated at a scale $\mathcal{M}^2$. Both diagrams in Fig. 3 are leading twist — they involve only one of the partons (a gluon and an antiquark, respectively) in the projectile, and one gluon in the target.
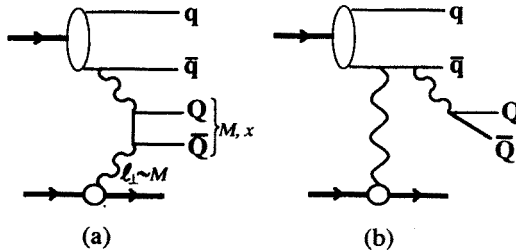

Fig. 3. Leading twist diagrams in heavy quark production at fixed momentum fraction x of the heavy pair. (a) A lowest order $GG \rightarrow Q\bar{Q}$ diagram. (b) A higher order $\bar{q}G \rightarrow \bar{q}Q\bar{Q}$ diagram. The gluons have virtualities ranging up to the mass scale $\mathcal{M}$ of the heavy pair. There is no restriction on the transverse size of the initial Fock state.

The dynamics of the new limit (4.1) differs in several respects from the above. There are two types of leading order diagrams, the "extrinsic" and "intrinsic" ones shown in Figs. 4(a) and (b), respectively. In extrinsic diagrams the heavy quark pair couples to only one parton in the projectile, while in intrinsic diagrams it couples to several. Since the produced $Q\bar{Q}$ pair carries almost all of the momentum in the final state ($x \rightarrow 1$), the light valence quarks $q, \bar{q}$ are effectively stopped. The light quarks then give a big contribution to the energy of the intermediate states, $2p\Delta E \sim p_\perp^2/(1-x)$ (*cf.* Eq. (2.3)). The production cross section is dominated by values of the light quark transverse momentum $p_\perp$ where this light quark contribution to the energy difference is of the same order as that of the heavy pair, $2p\Delta E \sim \mathcal{M}^2$. Hence (for $\mu \gtrsim \Lambda_{\text{QCD}}$)

$$p_\perp^2 \sim \mathcal{M}^2(1-x) = \mu^2 \,. \tag{4.3}$$

Because of their small fraction $\sim (1-x)$ of the projectile momentum, the stopped light quarks can move a considerable distance $R_\perp$ in the transverse direction, even during the brief life-time of the virtual $q\bar{q}Q\bar{Q}$ Fock state.

According to Eq. (2.6), $R_\perp \sim 1/p_\perp \sim 1/\mu$. Now a Fock state of this transverse size can be "resolved" by a target gluon of transverse momentum $\ell_\perp$ (or virtuality $\ell^2 \sim -\ell_\perp^2$) of order[2] $\ell_\perp \sim 1/\mu$. Hence the hardness of the scattering from the target does *not* increase with the heavy quark pair mass $\mathcal{M}$. To be able to describe the target scattering using PQCD, we would have to choose $\mu \gg \Lambda_{\text{QCD}}$ in the limit (4.1). In general, however, we must conclude that arbitrarily heavy quarks can be, and are, produced at high x by *soft* peripheral scattering. Such soft scattering is surface-dominated for nuclear targets, *i.e.*, $\sigma \propto A^{2/3}$ as observed for J/ψ production at large x (see below).

Note that soft scattering is kinematically allowed only at sufficiently high energies. The minimum longitudinal momentum transfer from a stationary target required to put a heavy quark pair of mass $\mathcal{M}$ on its mass shell is of order $\mathcal{M}^2/2p$, where p is the laboratory momentum of the projectile. For charm production the minimum momentum transfer is below 50 MeV already for $p > 100$ GeV.
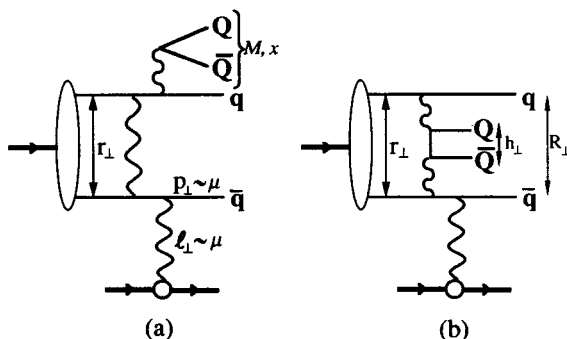

(a)   (b)

Fig. 4. Leading order diagrams in the limit (4.1). In the extrinsic diagram (a) the produced heavy quark pair couples directly to only one parton in the projectile. Diagram (b) is intrinsic, as the $Q\bar{Q}$ pair couples to two partons. In the standard limit (4.2), both diagrams (a) and (b) would be classified as higher twist, and would be suppressed by $1/\mathcal{M}^2$. The gluon from the target has a virtuality of $\mathcal{O}(\mu)$, while the two other gluons have virtualities of $\mathcal{O}(\mathcal{M})$. The transverse sizes $r_\perp$ and $R_\perp$ of the initial and final Fock states are as in Fig. 1, and the size of the $Q\bar{Q}$ pair is $h_\perp \sim 1/\mathcal{M}$.

The large transverse size $R_\perp$ of the light quark distribution also explains why the scattering dominantly occurs off the light quarks, as shown in

---

[2] Equivalently, we could say that an interaction of this hardness with the target deflects the stopped light quarks sufficiently to break up the Fock state and materialize the heavy quark pair.

Fig. 4. The heavy $Q\bar{Q}$ pair has a small transverse size $h_\perp \sim 1/\mathcal{M}$. A target gluon can couple to, and resolve[3], the $Q\bar{Q}$ pair only provided it has a commensurate wavelength, *i.e.*, $\ell_\perp \sim \mathcal{M}$ as indicated in Fig. 3(a). This is much larger than the $\ell_\perp \sim \mu$ required to resolve the light quarks. Hence the gluon fusion diagram of Fig. 3(a), which gives the leading contribution in the usual, fixed x, QCD limit (4.2), is actually suppressed by $1/\mathcal{M}$ compared to the diagrams of Fig. 4 in the new limit (4.1).

The Fock state of the projectile hadron from which the heavy pair is produced must have a small transverse size $r_\perp^2 \sim (1-x)/\mu^2 \sim 1/\mathcal{M}^2$ (*cf.* Fig. 4). The argument is the same as the one already given in Section 2, leading to the estimate (2.4) of the valence quark transverse momentum before the virtual creation of the heavy quark pair.

The extrinsic (Fig. 4(a)) and intrinsic (Fig. 4(b)) diagrams are of the same order in α_s and have the same behavior in the limit (4.1). However, we note some qualitative distinctions between these two classes of diagrams:
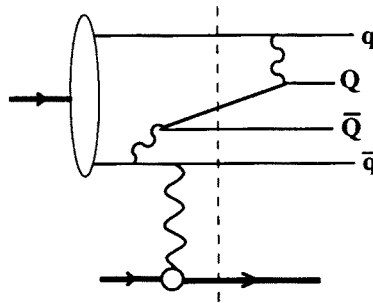

Fig. 5. In an intrinsic process the intermediate state indicated by the vertical dashed line can be on-shell, resulting in an imaginary part of the amplitude at leading order.

(i) The intrinsic diagrams do not contribute significantly to lepton pair production, since two photon exchanges would be required. This may explain the very different A-dependence of lepton pairs, as compared to the J/ψ (see below).

(ii) The intrinsic diagrams give rise to a non-trivial phase in the leading order amplitude. As shown in Fig. 5, in an intrinsic diagram the $Q\bar{Q}$ production can proceed through two consecutive real processes. First an on-shell $Q\bar{Q}$ pair with $x < 1$ is formed, and later the pair is accelerated to $x \to 1$ via an interaction with the second valence quark.

---

[3] If the virtual $Q\bar{Q}$ pair is in a color octet configuration it will also interact coherently with soft gluons. In this case the virtual pair behaves like pointlike gluon, and is not materialized.

This dynamical phase can be of importance in polarization phenomena, which have been observed [12, 13] to be enhanced at large x.

(iii) The extrinsic diagrams dominate over the intrinsic ones both in the exclusive ($\mu \ll \Lambda_{\text{QCD}}$ in Eq. (4.1)) and inclusive ($\mu \gg \Lambda_{\text{QCD}}$) limits. In the extrinsic diagram of Fig. 4(a), the virtuality of the gluon exchange between the light valence quarks is set by $1/r_\perp^2 \sim \Lambda_{\text{QCD}}^2/(1-x)$, while that of the gluon connecting to the heavy quark pair is set by $\mathcal{M}^2$. In the intrinsic diagram of Fig. 4(b), on the other hand, *both* gluons have virtualities determined by the *larger* of these scales. In the scalar QED model calculation of Ref. [2], the intrinsic diagrams nevertheless dominated at intermediate values of μ^2. It would clearly be important to determine the magnitude of the intrinsic contribution in QCD.

5. The production of charmed hadrons at large x

The data on charm production in e^+e^- annihilations [14] and in photoproduction [15] agrees well with PQCD at leading twist. The charm fragmentation function $D(\text{c} \to \text{D} + X)$ can thus be determined from these reactions using the factorization formula (1.1). The e^+e^- data show [16] that the charmed hadron carries an average fraction $\langle z \rangle \simeq 70\%$ of the charm quark momentum. The momentum distribution is often parametrized in terms of the "Peterson" function [17],

$$D_{H/\text{c}}(z) \propto \frac{1}{z(1 - 1/z - \epsilon_{\text{c}}/(1-z))^2}, \tag{5.1}$$

where $\epsilon_{\text{c}} \simeq 0.06$. According to the QCD factorization theorem, this fragmentation function should be the same in all hard processes, regardless of how the charm quark is produced.

There are several experiments on hadroproduction of charm [18–22] which give much larger cross sections at high x than expected from leading twist QCD, *i.e.*, from Eq. (1.1) with a fragmentation function of the form (5.1). Recently, data with good statistics on $\pi^- A \to \text{D} + X$ [23, 24] clearly shows that Eq. (1.1) underestimates the charm cross section already at medium values of $x \gtrsim 0.2$. As shown in Fig. 6(a), the experimental D-meson distribution actually is similar to that predicted by Eq. (1.1) for the charm *quark* [23, 25]. Thus the fragmentation function $D(\text{c} \to \text{D} + X)$ must be assumed to be close to $\delta(1 - z)$ in order to get agreement between experiment and theory in charm hadroproduction at medium x. Hadroproduced charm quarks appear to fragment in a strikingly different way from what they do in e^+e^- annihilations, where the fragmentation function is to a good approximation given by Eq. (5.1). This implies a breakdown of the leading twist factorization formula (1.1).
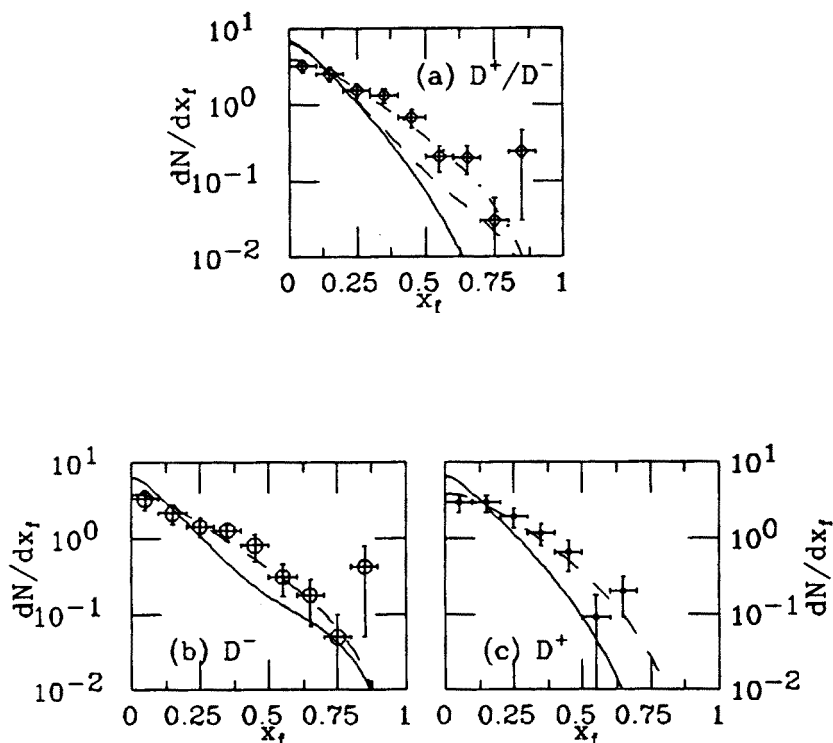
Fig. 6. x_F distributions [25] of D mesons produced in π^-A collisions at 250 GeV/c (E769 data [23]). (a) The solid line shows the prediction of leading twist QCD, using a Peterson [17] fragmentation scheme for $c \to D + X$ which fits the data on D production in e^+e^- annihilations. The dashed curve shows the effect of adding an estimated intrinsic charm contribution to the fusion cross section. The dot-dashed curve results from fusion + intrinsic charm at the quark level, *i.e.*, for δ-function fragmentation. (b) D^- production, for which the curves include both the fusion and intrinsic production mechanisms. The solid curve is obtained with Peterson fragmentation and the dashed curve with δ-function fragmentation. (c) As in (b), for D^+ production.

The different form of the fragmentation function in e^+e^- induced, compared to hadron induced, charm production has a natural explanation [25, 26]. In hadroproduction, the charm quark can coalesce with light spectator quarks from the projectile, which move in the same direction and with similar velocity as the charm quark. The charmed hadron formed this way will have the same velocity as the charm quark, resulting in a fragmentation

function close to the δ-function suggested by the data.

The existence of coalescence between charm quarks and light valence quarks from the projectile is suggested also by the "leading particle effect". Those charmed hadrons that have a valence quark in common with the projectile are experimentally found [23, 24, 27] to have a harder x-distribution. In Fig. 6(b),(c) we show the size of this effect as measured by E769 [23], and as expected in a model with coalescence [25]. From this model one can also see that the E769 data is not very sensitive to the estimated contribution of intrinsic charm, which is important only at the highest values of x.

6. The A dependence of quarkonium production

The coalescence of heavy quarks with light comovers has an indirect effect on the production of quarkonium states, such as the J/ψ and Υ. When many comoving light quarks are present, as in the fragmentation region of heavy nuclei, the heavy quarks may preferentially coalesce with comovers rather than bind to each other [26]. This leads to a suppression of quarkonium production in nuclear fragmentation regions, which has been observed for the J/ψ in central heavy ion collisions [28]. A similar suppression is also observed in "backward" ($x < 0$) production of both the J/ψ and the Υ in pA collisions [29], for which the alternative explanation [30] in terms of a quark gluon plasma seems unlikely.

The forward ($x > 0$) production of the J/ψ has been measured with high statistics for both pion and proton beams on a variety of nuclear targets [31–33]. In this case the effect of coalescence should be small, since the $c\bar{c}$ state is produced in the fragmentation region of a hadron, and has relatively few comovers. This data nevertheless gives direct evidence [34] for the breakdown of the leading twist approximation at large x. In the factorized formula (1.1), the nuclear target A-dependence can only appear through the target structure function $F_{b/A}(x_2)$, where x_2 is the momentum fraction carried by the target parton b. Ratios of J/ψ cross sections at different production energies but at the same x_2 should therefore be independent of the nuclear number A. As shown in Fig. 7 for the NA3 data [31] on $\pi^- A \to J/\psi + X$ at 150 and 280 GeV, the ratio of cross sections on Hydrogen and Platinum does not in fact scale as a function of x_2. Thus the leading twist factorization (1.1) fails. A similar result was obtained by combining pA data from NA3 and E772 [33].

The failure of factorization occurs at the smallest values of x_2, *i.e.*, for large Feynman x of the J/ψ, since $x_2 \simeq M_{J/\psi}^2/xs$. In this region of x the nuclear target dependence of the J/ψ cross section also is not linear in A, as expected for hard QCD processes which occur incoherently off all partons
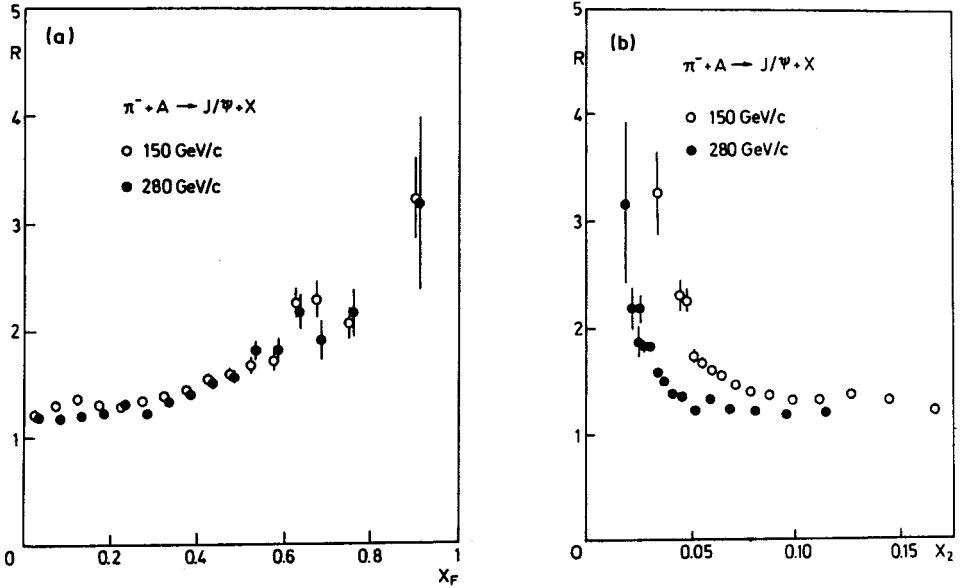
Fig. 7. The ratio $R = A\sigma(pp \to J/\psi + X)/\sigma(pA \to J/\psi + X)$ of inclusive J/ψ production cross sections on Hydrogen and Platinum [31]. In (a) the ratio is plotted as a function of the Feynman x_F of the J/ψ, and in (b) as a function of the momentum fraction x_2 of the target parton [34].

in the nucleus. If the J/ψ cross section is parametrized as

$$\sigma_{hA} = \sigma_{hN} A^\alpha , \qquad (6.1)$$

one finds [31–33] that $\alpha = 0.7 \ldots 0.8$.

At small values of x_2, one does expect $\alpha \lesssim 1$ due to parton shadowing [35], as observed [36] in deep inelastic lepton scattering (DIS) and in lepton pair production (DY). However, shadowing appears to be a Q^2-independent, leading twist effect associated with the nuclear structure function. It thus cannot account for the breakdown of factorization observed in J/ψ production. Moreover, the shadowing effect seen in DIS and in DY is a fairly small, $10 \ldots 30\%$ effect, whereas the suppression of J/ψ production amounts to a factor ~ 3 for large nuclei.

It was recently suggested [37–39] that the nuclear suppression of J/ψ production could be due to energy loss of the incoming and outgoing partons while propagating through the nucleus. However, very little energy loss is observed for the struck quark in the DIS process [40], as well as for the incoming quark in the DY reaction [41]. This shows that high energy

quarks suffer only insignificant energy loss in the nucleus. Actually, this fact is a direct consequence of the uncertainty principle, which forbids enhanced energy loss from multiple collisions occurring within the formation zone of the radiated gluons [42]. Repeated radiation from collisions separated by a time interval Δt is allowed only provided $\Delta E \Delta t \gtrsim 1$, *i.e.*, when the energy difference resulting from the gluon radiation ΔE is big enough for the multiple scatterings to be resolved. In a nucleus, $\Delta t \lesssim R_A$, where R_A is the nuclear radius. The emission of a gluon with transverse momentum $p_\perp$ and energy E_g results in $\Delta E \simeq p_\perp^2/2E_g$. Hence normal, soft collisions in the nucleus with $\langle p_\perp^2 \rangle \sim 0.1$ GeV^2 can only lead to a *finite* energy loss in the laboratory frame,

$$E_g \lesssim \tfrac{1}{2} \langle p_\perp^2 \rangle R_A \lesssim 1.5 \text{ GeV}. \tag{6.2}$$

For high energy partons this fixed energy loss is not significant, and it cannot explain the nuclear suppression of J/ψ production.

When the fixed energy loss (6.2) is small compared to the energy of the J/ψ, we expect to see Feynman scaling (in x) of the J/ψ cross section. This is indeed observed in the data (*cf.* Fig. 7). Hence it is most natural to discuss the J/ψ x-distribution from the point of view of the projectile wave function. This brings us back to our earlier discussion of heavy quark production at large x. The A-dependence of the J/ψ data is indeed one of the strongest arguments for the relevance of the new QCD limit (4.1), where $\mathcal{M}^2(1-x)$ is held fixed as $\mathcal{M}^2 \to \infty$ and $x \to 1$.

In Section 4 we saw that a virtual heavy quark pair with x near 1 can be put on its mass shell (produced) by a soft gluon scattering off the stopped light quarks. If $1 - x = \mu^2/\mathcal{M}^2$, the light quark distribution has a transverse size $1/\mu$, and the hardness of the target interaction is $Q^2 = \mu^2$ (*cf.* Eq. (4.3)). Hence for small $\mu \sim \Lambda_{\text{QCD}}$, the scattering will be surface-dominated in a big nucleus, and the cross section gets an $A^{2/3}$ nuclear target dependence. There should thus be a smooth transition from an A^1 behavior at small x (hence large μ) to an $A^{2/3}$ behavior at large x, in agreement [43] with the data.

The NA3 data [31] was analyzed assuming the existence of two components in the cross section, a "hard" component with $\alpha = 0.972$ in (6.1) and a "diffractive" component with $\alpha = 0.77$ (for the $\pi^- A$ data) or $\alpha = 0.71$ (for the pA data). A quantitative fit showed that the hard component was in good agreement with expectations from the GG $\to c\bar{c}$ and $q\bar{q} \to c\bar{c}$ fusion processes. Hence the "diffractive" component, which dominates for $x \gtrsim 0.6$, appears to be an excess over the leading twist QCD fusion contribution. Note that explanations of the anomalous nuclear dependence in terms of energy loss or breakup of the J/ψ would not lead to any excess in the large x production cross section on light targets.

Because the target interaction in the $x \to 1$ limit (4.1) can be soft ($\ell_\perp \sim \mu$ in Fig. 4), the average transverse momentum $\langle k_\perp \rangle$ of the J/ψ should decrease from $\langle k_\perp \rangle = \mathcal{O}(m_c)$ at low x to $\langle k_\perp \rangle = \mathcal{O}(\mu)$ at large x. This effect has been seen in the J/ψ data [12]. Furthermore, the anomalous A-dependence, $i.e.$, $\alpha < 1$ in Eq. (6.1), is observed [31, 32] only at low $k_\perp$. A similar decrease of $\langle k_\perp \rangle$ with x is expected also in open charm production. In addition, coalescence between heavy and light quarks occurs mainly for heavy quarks with low $k_\perp$, comparable to the light quark transverse momenta. This also tends to decrease the $\langle k_\perp \rangle$ of charmed hadrons at large x.

For Υ production, the available data is not at large enough x to make $\mu^2 = (1 - x)\mathcal{M}^2$ small. Hence the corrections to the leading twist results should not be very significant. The A-dependence of the Υ cross section is in fact found [29] to be much closer to A^1 than is the case for the J/ψ.

7. Concluding remarks

We have discussed the corrections to the twist expansion of PQCD for hard processes in the kinematic region where some of the constituents (or hadrons) carry a large fraction $x \to 1$ of the available energy. We found that the limit (1.2), where the hard scale Q^2 (or $\mathcal{M}^2$) is comparable to the scale $\Lambda_{\mathrm{QCD}}^2/(1 - x)$, is particularly interesting. The production mechanism of a heavy quark pair of mass $\mathcal{M}$ becomes peripheral in this limit, with the hardness μ^2 of the target interaction being given by $\mu^2 = \mathcal{M}^2(1 - x)$. For $\mu \lesssim \Lambda_{\mathrm{QCD}}$ this means that the interaction in the target is soft. In this situation the factorization formula (1.1), according to which the scattering occurs incoherently off single partons in the target, breaks down. In particular, it implies scattering from the surface of large nuclei, and a consequent $A^{2/3}$ nuclear target dependence.

On the other hand, only very compact Fock states of the projectile, where the transverse separation of the light valence quarks is of order $1/\mathcal{M}$, can participate in the production. For large x *several* valence partons of the projectile are involved in the heavy quark production process, again breaking the leading twist, single parton factorization (1.1). In this respect the dynamics is similar to that in the exclusive ($x = 1$) limit. The hard production vertex can be calculated in PQCD, given the longitudinal momentum distributions of the quarks in the transversally compact Fock states of the projectile. So far, this calculation has only been carried out [2] in a scalar QED model, however.

Phenomenologically, significant deviations from the leading twist approximation have been seen at large x in deep inelastic lepton scattering [7], in lepton pair production [9, 10], in J/ψ hadroproduction [31–33] and in

open charm hadroproduction [18–22]. Recently, firm evidence was obtained [23, 24] that there are significant corrections to the leading twist PQCD cross section for open charm hadroproduction even at moderate $x \gtrsim 0.2$. The most natural explanation for this effect is the coalescence of the charm quark with co-moving light spectator quarks [25, 26]. Coalescence is a soft process, which is not directly calculable in PQCD. It allows the charm quark to maintain its velocity during hadronization, and can thus effectively be described by a fragmentation function $D(z) \simeq \delta(1 - z)$.

A significant change in the velocity of a heavy quark always requires large momentum transfer — hence this is a process that is associated with the hard production vertex, not with soft hadronization. Some fragmentation schemes based on the string model [44,45] give rise to charmed hadron distributions which are considerably harder than the distribution of the charm quark [22, 24]. Such mechanisms seem to go beyond the realm of soft physics for which the models were intended, and are thus unreliable. The methods that we have described above illustrate how the cross section of heavy quark production at the largest values of x can be calculated in QCD. While the size of the new, intrinsic contributions to charm production has not yet been determined from the theory, phenomenological estimates [25, 43] show that they are important for $x \gtrsim 0.5$. Several experiments have in fact reported larger charm hadroproduction cross sections at high x than would be expected from the leading twist approximation (1.1). These data await confirmation by upcoming, high statistics experiments.

REFERENCES

[1] J.C. Collins, D.E. Soper, G. Sterman, published in *Perturbative QCD*, ed. A.H. Mueller, World Scientific, 1989; G. Bodwin, *Phys. Rev.* **D31**, 2616 (1985); *Phys. Rev.* **D34**, 3932 (1986E); J. Qiu, G. Sterman, *Nucl. Phys.* **B353**, 105 (1991), *Nucl. Phys.* **B353**, 137 (1991).

[2] S.J. Brodsky, P. Hoyer, A. H. Mueller, W.-K. Tang, *Nucl. Phys.* **B369**, 519 (1992).

[3] S.J. Brodsky, G.P. Lepage, published in *Perturbative QCD*, ed. A.H. Mueller, World Scientific, 1989.

[4] D. Sivers, S.J. Brodsky, R. Blankenbecler, *Phys. Rep.* **23C**, 1 (1976).

[5] J.F. Gunion, P. Nason, R. Blankenbecler, *Phys. Rev.* **D29**, 2491 (1984).

[6] S.J. Brodsky, I. Schmidt, *Phys. Lett.* **B234**, 144 (1990).

[7] M. Virchaux, A. Milsztajn, *Phys. Lett.* **B274**, 221 (1992).

[8] M. Soldate, *Nucl. Phys.* **B223**, 61 (1983).

[9] S. Falciano, *et. al.*, *Z. Phys.* **C31**, 513 (1986); *Z.Phys.* **C37**, 545 (1988).

[10] J.S. Conway, *et. al.*, *Phys. Rev.* **D39**, 92 (1989).

[11] E.L. Berger, S.J. Brodsky, *Phys. Rev. Lett.* **42**, 940 (1979); S.S. Agaev, *Phys. Lett.* **B283**, 125 (1992).

[12] C. Biino et al., *Phys. Rev. Lett.* **58**, 2523 (1987).

[13] D.L. Adams, *et. al.*, *Phys. Lett.* **B261**, 201 (1991); *Phys. Lett.* **B264**, 462 (1991).

[14] M. Derrick, *Proceedings of the XXIV International Conference on High Energy Physics*, Eds. R. Kotthaus and J. H. Kühn, Springer 1989, p. 895.

[15] J.C. Anjos, *et. al.*, *Phys. Rev. Lett.* **62**, 513 (1989).

[16] S. Bethke, *Z. Phys.* **C29**, 175 (1985); W. Bartel, *et. al.*, *Z. Phys.* **C33**, 339 (1987); J. Chrin, *Z. Phys.* **C36**, 163 (1987); D. Decamp, *et. al.*, *Phys. Lett.* **244B**, 551 (1990).

[17] C. Peterson, D. Schlatter, I. Schmitt, P. Zerwas, *Phys. Rev.* **D27**, 105 (1983).

[18] S.F. Biagi, *et. al.*, *Z. Phys.* **C28**, 175 (1985).

[19] P. Chauvat, *et. al.*, *Phys. Lett.* **199B**, 304 (1987).

[20] P. Coteus, *et. al.*, *Phys. Rev. Lett.* **59**, 1530 (1987).

[21] C. Shipbaugh, *et. al.*, *Phys. Rev. Lett.* **60**, 2117 (1988).

[22] M. Aguilar-Benitez, *et. al.*, *Z. Phys.* **C40**, 321 (1988).

[23] J.A. Appel, FERMILAB-Pub-92/49, to appear in *Ann. Rev. Nucl. Part. Sci.* **42** (1992); G.A. Alves, *et. al.*, FERMILAB-Pub-92/208-E, August 1992; Contribution to ICHEP 92, Dallas, Texas, August 1992.

[24] M. Adamovich, *et. al.*, WA82 Collaboration, Contribution to ICHEP 92, Dallas, Texas, August 1992.

[25] R. Vogt, S.J. Brodsky, P. Hoyer, SLAC-PUB-5827, to be published in *Nucl. Phys. B*.

[26] S. J. Brodsky, A.H. Mueller, *Phys. Lett.* **206B**, 285 (1988); R. Vogt, S. Gavin, *Nucl. Phys.* **B345**, 104 (1990).

[27] M. Aguilar-Benitez et al., *Phys. Lett.* **161B**, 400 (1985); *Z. Phys.* **C31**, 491 (1986); S. Barlag et al., *Z. Phys.* **C49**, 555 (1991).

[28] C. Baglin, *et. al.*, *Phys. Lett.* **220B**, 471 (1989).

[29] D.M. Alde, *et. al.*, *Phys. Rev. Lett.* **66**, 2285 (1991); M.J. Leitch, *et. al.*, *Nucl. Phys.* **A544**, 197c (1992).

[30] T. Matsui, H. Satz, *Phys. Lett.* **B178**, 416 (1986).

[31] J. Badier et al., *Z. Phys.* **C20**, 101 (1983).

[32] S. Katsanevas et al., *Phys. Rev. Lett.* **60**, 2121 (1988).

[33] D.M. Alde et al., *Phys. Rev. Lett.* **66**, 133 (1991).

[34] P. Hoyer, M. Vänttinen, U. Sukhatme, *Phys. Lett.* **246B**, 217 (1990).

[35] For discussions of nuclear structure function shadowing in QCD, see, *eg.*, L.L. Frankfurt, M.I. Strikman, *Nucl. Phys.* **B316**, 340 (1989); A.H. Mueller, J.-W. Qiu, *Nucl. Phys.* **B268**, 427 (1986); S.J. Brodsky, H.J. Lu, *Phys. Rev. Lett.* **64**, 1342 (1990); V. Barone, M. Genovese, N. N. Nikolaev, E.Predazzi, B. G. Zakharov, University of Torino preprint DFTT 14/92.

[36] M. Arneodo, CERN-PPE/92-113, June 1992, submitted to *Phys. Rep.*.

[37] S. Gavin, J. Milana, *Phys. Rev. Lett.* **68**, 1834 (1992).

[38] E. Quack, Heidelberg preprint HD-TVP-92-2, June 1992.

[39] S. Frankel, W. Frati, University of Pennsylvania preprint UPR-0499T, May 1992.

[40] EMC Collaboration, A. Arvidson *et. al.*, *Nucl. Phys.* **B246**, 381 (1984); R. Windmolders, *Proceedings of the 24 International Conference on High Energy Physics, Munich 1988*, eds. R. Kotthaus and J. H. Kühn, Springer, 1989, p. 267.

[41] D. M. Alde *et. al.*, *Phys. Rev. Lett.* **64**, 2479 (1990).

[42] S.J. Brodsky, P. Hoyer, SLAC-PUB-5935, September 1992, submitted to *Phys. Lett. B.*

[43] R. Vogt, S.J. Brodsky, P. Hoyer, *Nucl. Phys.* **B360**, 67 (1991).

[44] H.-U. Bengtsson, G. Ingelman, *Comput. Phys. Commun.* **34**, 231 (1985).

[45] H.-U. Bengtsson, T. Sjöstrand, *Comput. Phys. Commun.* **46**, 43 (1987).